

Available online at www.sciencedirect.com

SciVerse ScienceDirect

journal homepage: www.elsevier.com/locate/watres

Activity of metazoa governs biofilm structure formation and enhances permeate flux during Gravity-Driven Membrane (GDM) filtration

Nicolas Derlon^{a,*}, Nicolas Koch^a, Bettina Eugster^c, Thomas Posch^c, Jakob Pernthaler^c, Wouter Pronk^a, Eberhard Morgenroth^{a,b}

^a Eawag: Swiss Federal Institute of Aquatic Science and Technology, Überlandstrasse 133, CH-8600 Dübendorf, Switzerland

^b Institute of Environmental Engineering, ETH Zürich, CH-8093 Zürich, Switzerland

^c Limnological Station, Institute of Plant Biology, University of Zürich, CH-8802 Kilchberg, Switzerland

ARTICLE INFO

Article history:

Received 2 August 2012

Received in revised form

17 January 2013

Accepted 20 January 2013

Available online 4 February 2013

Keywords:

Biofilm structure

GDM system

Bacterial growth capacity

Metazoa

Flux stabilization

ABSTRACT

The impact of different feed waters in terms of eukaryotic populations and organic carbon content on the biofilm structure formation and permeate flux during Gravity-Driven Membrane (GDM) filtration was investigated in this study. GDM filtration was performed at ultra-low pressure (65 mbar) in dead-end mode without control of the biofilm formation. Different feed waters were tested (River water, pre-treated river water, lake water, and tap water) and varied with regard to their organic substrate content and their predator community. River water was manipulated either by chemically inhibiting all eukaryotes or by filtering out macrozoobenthos (metazoan organisms). The structure of the biofilm was characterized at the meso- and micro-scale using Optical Coherence Tomography (OCT) and Confocal Laser Scanning Microscopy (CLSM), respectively. Based on Total Organic Carbon (TOC) measurements, the river waters provided the highest potential for bacterial growth whereas tap water had the lowest. An increasing content in soluble and particulate organic substrate resulted in increasing biofilm accumulation on membrane surface. However, enhanced biofilm accumulation did not result in lower flux values and permeate flux was mainly influenced by the structure of the biofilm. Metazoan organisms (in particular nematodes and oligochaetes) built-up protective habitats, which resulted in the formation of open and spatially heterogeneous biofilms composed of biomass patches. In the absence of predation by metazoan organisms, a flat and compact biofilm developed. It is concluded that the activity of metazoan organisms in natural river water and its impact on biofilm structure balances the detrimental effect of a high biofilm accumulation, thus allowing for a broader application of GDM filtration. Finally, our results suggest that for surface waters with high particulate organic carbon (POC) content, the use of worms is suitable to enhance POC removal before ultrafiltration units.

© 2013 Elsevier Ltd. All rights reserved.

* Corresponding author. Tel.: +41 448235378.

E-mail address: nicolas.derlon@eawag.ch (N. Derlon).

0043-1354/\$ – see front matter © 2013 Elsevier Ltd. All rights reserved.

<http://dx.doi.org/10.1016/j.watres.2013.01.033>

1. Introduction

Gravity-Driven Membrane (GDM) filtration is increasingly used for the production of drinking water in developing and transient countries. GDM filtration represents a new and relevant alternative compared to conventional membrane filtration for which significant amounts of energy and chemicals are used in order to control the biofilm formation. GDM filtration is performed at low transmembrane pressure (less than 0.1 bar) using a simple set-up (Arnal et al., 2008; Butler, 2009; Peter-Varbanets et al., 2010). Most of the current GDM systems are operated with pre- or post treatment of the water and with control of the biofilm formation (Arnal et al., 2008; Butler, 2009). The operation of these GDM systems thus required some energy, maintenance effort and a specific knowledge (Arnal et al., 2008; Butler, 2009).

GDM ultrafiltration without any control of the biofilm formation (no flushing, no backwashing, and no chemical cleaning) was recently reported (Peter-Varbanets et al., 2010). Biofilm formation on membrane surfaces during GDM filtration results from the structured aggregation of biomass and from the accumulation of particulate matter. The development of a highly permeable biofilm on membrane surfaces allowed for the long-term operation (several years) of the system at a stable flux ranging from 4 to 10 L m⁻² h⁻¹. The stabilization of the permeate flux indicated no or very low biofouling of the membrane. However, two key questions need to be answered prior to a broader application of GDM filtration: (1) What are the mechanisms responsible for flux stabilization? (2) Which factors influence the level of flux stabilization?

Microbial activity has been shown to be a key factor leading to flux stabilization. A continuous permeate flux decline was observed when GDM filtration was performed after inhibition of all organisms (using sodium azide) (Peter-Varbanets et al., 2010). Furthermore, it has been shown that a higher Total Organic Carbon (TOC) content in the feed water resulted in a lower level of flux stabilization (Peter-Varbanets et al., 2010). However, we have shown that the level of flux stabilization can be increased by predation: Highly permeable biofilms characterized by an open and heterogeneous structure develop in presence of predators (Derlon et al., 2012). Flat and compact biofilms associated with a low permeate flux were observed in absence of predation (inhibited by using a eukaryote-specific antibiotic). However, in this study the eukaryotic populations responsible for the increase of the biofilm permeability were not identified, as both, unicellular protists and larger metazoa were inhibited. In natural biofilms, metazoa significantly influence the biofilm structure formation. Metazoa such as nematodes first create and then live in protective habitats, which results in the formation of patchy and heterogeneous biofilms (Riemann and Helmke, 2002). The same process was also reported for larger organisms such as larvae (Stief and Becker, 2005). If metazoa can engineer the biofilm structure, it can be hypothesized that these organisms are also responsible for the formation of heterogeneous and open biofilms on membrane surfaces observed during GDM filtration of surface water. Also, it is still unclear to which extent predation by higher organisms can balance high bacterial

growth capacity and maintain high stable flux during GDM filtration. As a basis for more robust control of GDM filtration, the contribution of each group of predators (protists and metazoa) has to be separately evaluated, as well as the capacity of predation to increase the permeability of biofilms that develop at higher total organic carbon (TOC) content in the feed water.

The objectives of this study were: (i) to identify the specific influence of protists and metazoan organisms on biofilm structure formation and on filtration performances, (ii) to evaluate the effect of particulate organic matter (in terms of TOC content) in the feed water on the biofilm structure formation and on filtration performances and (iii) to evaluate to what extent predation can increase permeability of biofilms developed at high TOC content in the feed water. Even though both protists and metazoa are predators of bacteria, we hypothesize that they will play different roles in biofilm structure formation due to their differences in (i) size, (ii) motility, (iii) affinities for food resources, and (iv) capability to engineer habitats. GDM filtration was evaluated with different feed water sources characterized by different TOC and predator composition (i.e., river, lake, and tap waters). Long-term dead-end filtration experiments were performed monitoring total amount and spatial distribution of the biofilm in combination with monitoring permeate flux and bacterial growth capacity.

2. Materials and methods

2.1. Operating conditions and water sources

Five different types of water sources characterized by different bacterial growth conditions and different predator diversity were evaluated (Table 1).

Three systems were fed with river water from the Chriesbach river (Dübendorf, Switzerland) with water temperature controlled at 20 °C using a submersible heater. In the River-W case, the system was operated without influencing the predator community. In this case, protists and metazoa were continuously added to the system and contributed to the development of the biofilm structure. For the River-Pre case, the river water was filtered through filter papers with a pore size ranging from 12 to 25 µm (Whatman, Maidstone, UK) to remove most of the metazoa. Protists are smaller than metazoa and pass through the pre-filter. In the River-Inhib case, both protists and metazoa were inhibited using cycloheximide (Sigma–Aldrich Chemie GmbH, Buchs, Switzerland). Lake water from taken from Lake Zurich (Switzerland) was used in the Lake-W case. In the Tap-W case, the system was operated with drinking water from the distribution system of the water supply of Dübendorf (Switzerland). We hypothesized that tap water was characterized by the absence of predators and by very low bacterial growth capacity.

2.2. Experimental setup

The experimental setups used in this study are shown in Fig. 1. For experiments run with river and lake waters, the water was continuously fed to storage tanks in which the

Table 1 – Details of the five different water sources used in this study in terms of protists, metazoan and TOC content.

Water type	Label	Water characteristics			Comments
		Protist content	Metazoa content	TOC content (mg TOC L ⁻¹)	
River water	River-W	Present	Present	2.5–3	Natural protistan and metazoan community
River water pre-filtered	River-Pre	Present	Removed	2.5–3	Pre-filtration of water at 12–25 µm to remove metazoa
River water with eukaryotic inhibition	River-Inhib	Inhibited	Inhibited	2.5–3	Inhibition of both protistan and metazoan organisms by using eukaryote-specific antibiotic
Lake water	Lake-W	Present	Present	1.5–2	Natural protistan and metazoan community
Tap water	Tap-W	Present at extremely low abundance	Absent	<0.5	Poor protistan and metazoan community and low growth capacity

water level was kept constant by means of an overflow (Fig. 1a). The Hydraulic Residence Time (HRT) in the storage tank was around 2 h. In experiments with pre-filtered river water or tap water, a recirculation tank was connected to the water tank (Fig. 1b). The overall HRT in these two tanks was one day and a peristaltic pump was used to recirculate water from the lower tank to the main tank. In experiments with inhibition of predators, a peristaltic pump was used to continuously inject cycloheximide solution between the storage tank and the filtration modules (dashed line, Fig. 1a). Storage tanks were connected to standard polycarbonate filter holders with an inner diameter of 48 mm (Whatman, Maidstone, Kent, UK) using silicon tubing (Saint-Gobain®, France). A distance of 65 cm was maintained between the water level in the storage tank and the membrane surface resulting in a transmembrane pressure of 65 mbar. The water tanks and tubes were cleaned every week to remove settled and attached biomass. The permeate water of each module was collected in plastic bottles at daily intervals.

Polyethersulfone ultrafiltration membranes (PBHK, Biomax Millipore, Billerica, MA, USA) with a nominal cutoff of 100 kDa were used with the exception of the system fed

with pre-filtered Chriesbach water where a polysulfone ultrafiltration membrane with a similar cutoff was used (Microdyn-Nadir GmbH, Wiesbaden, Germany). Polysulfone membranes were initially tested with normal river water and no differences with polyethersulfone membranes were observed in terms of biofilm structure and permeation. Prior to utilization, membranes were stored in deionized water for at least 24 h to remove conservation agents and other chemicals. The deionized water was renewed several times during this washing. The hydraulic resistance of the new membranes was evaluated by filtering 1 L of deionized water under 65 mbar.

2.3. Cycloheximide injection

Cycloheximide solution at a concentration of 1.5 g L⁻¹ was injected in the modules using a peristaltic pump (Ismatec SA, Glattbrugg, Switzerland). The injection was performed discontinuously (15 min pumping, 60 min break). The flow rate (around 50 mL d⁻¹) was adjusted to the measured filtration flux to reach an appropriate concentration of 100 mg L⁻¹ in the feed water.

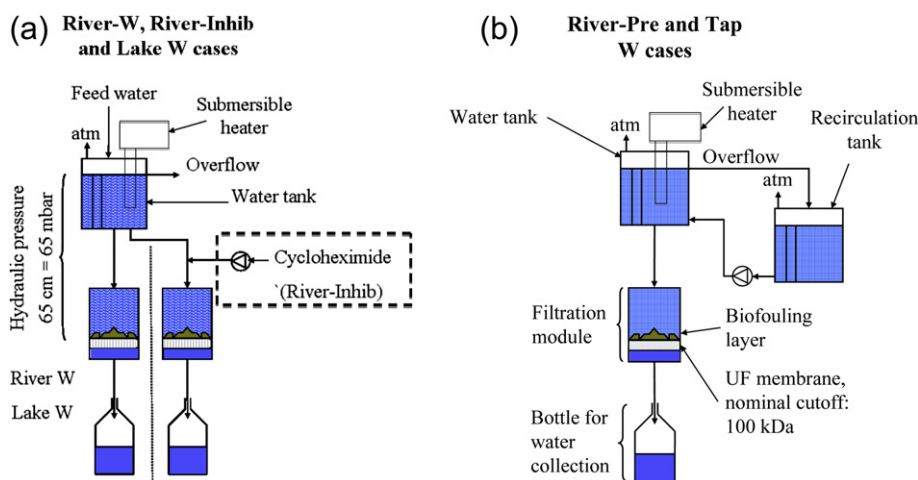


Fig. 1 – Schematic representation of the gravity-driven dead-end UF system including the water tank, the recirculation tank (Tap-W and River-Pre cases, 1b), the cycloheximide injection (River-Inhib case, 1a, dashed line), the filtration module containing the UF membrane (100 kDa) and the bottle for permeate collection.

2.4. Characterization of the biofilm structure

2.4.1. Top view pictures and membrane coverage

Top view pictures were used to get information about the overall morphology of the biofilms at a macroscopic scale (i.e., the fraction of the membrane surface that is covered by biofilms, Fig. 3). Top view pictures of the biofilms were recorded using a digital photo camera (Olympus C-7070, Le Mont-sur-Lausanne, Switzerland). For the image acquisition, filtration modules were opened and carefully placed on a stage. Top view pictures were then acquired and processed using ImageJ (<http://rsb.info.nih.gov/ij/>) to quantify the membrane coverage. First, the images were converted into 8-bits pictures. An automatic threshold (determined using the triangle method) was applied to binarize the images. According to our experiences, the triangle algorithm was the more accurate thresholding method based on visual observations and in order to distinguish the relevant structures, i.e., the biofilm and the uncovered membrane. The effective surface of the membrane was finally selected to calculate the membrane coverage.

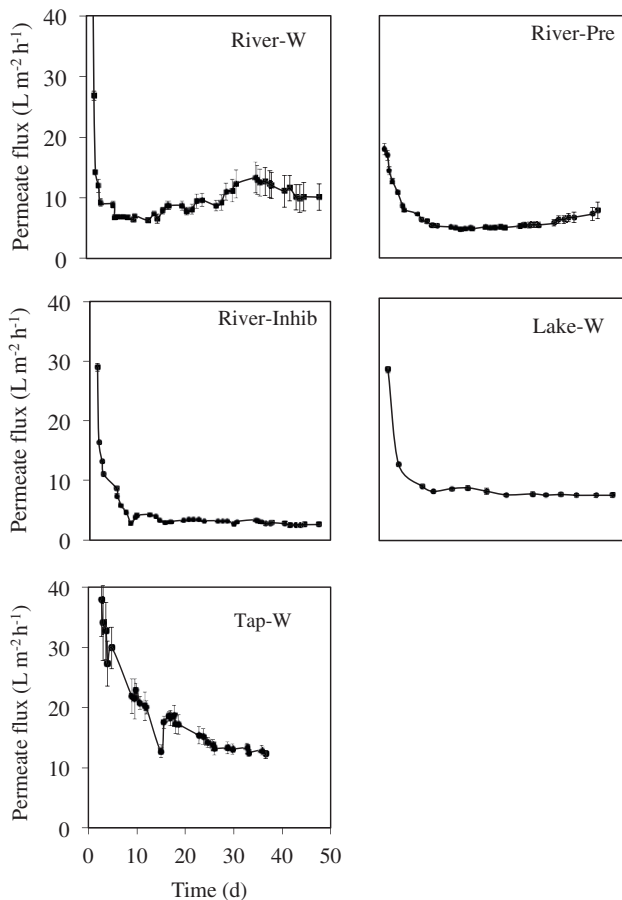


Fig. 2 – Change in the mean fluxes ($\text{L m}^{-2} \text{h}^{-1}$) measured for the different types of water and over 50 days of filtration. The standard errors are shown as error bars. Explanation of experimental conditions are provided in Table 1.

2.4.2. Optical coherence tomography

Optical Coherence Tomography (OCT) (model 930 nm Spectral Domain, Thorlabs GmbH, Dachau, Germany) with a central light source wavelength of 930 nm was used to investigate the meso-scale structure of the biofilm. The use of long wavelength light allows to penetrate up to a depth of 2.7 mm (in air, i.e., with a refractive index of 1) with axial and lateral resolutions of 4.4 μm and 15 μm , respectively. For the image acquisition, filtration modules were opened and carefully placed on the OCT stage. OCT images were recorded keeping the samples immersed in a thin layer of permeate. Around 20 images of biofilm cross sections (either 5 mm \times 1 mm, 5 mm \times 0.5 mm, or 3 mm \times 0.5 mm, depending of the biofilm thickness) were acquired at different time intervals and for each filtration module. Image analysis software developed under Matlab[®] (MathWorks, Natick, US) was used to analyse OCT images. Image analysis consisted of the following steps:

- (1) detecting the membrane–biofilm interface (filtering followed by grey-scale gradient analysis);
- (2) binarizing the image (automatic thresholding using Triangle algorithm);
- (3) calculating physical properties of the biofilm: mean biofilm thickness (in μm), absolute (R_a in μm) and relative roughness (R_a') coefficients.

These parameters were calculated according the following equations:

$$\bar{Z} = \frac{1}{n} \sum_{i=1}^N Z_i \quad (1)$$

$$R_a = \frac{1}{N} \sum_{i=1}^N (|Z_i - \bar{Z}|) \quad (2)$$

$$R_a' = \frac{1}{N} \sum_{i=1}^N \left(\left| \frac{Z_i - \bar{Z}}{\bar{Z}} \right| \right) \quad (3)$$

Linear regression analysis was performed to statistically evaluate the effect of the level of predation on the biofilm physical structure (membrane coverage, mean biofilm thickness and relative roughness coefficient). Only the biofilms developed in GDM systems operated with river waters were considered for this analysis. The linear least square function of R (R Development Core Team, 2011) version 2.13.0 was used to fit the model. This approach consisted in comparing the slopes of the change in the membrane coverage (or biofilm thickness or relative roughness) to the slopes estimated for a reference case (River-W). First-order equations with qualitative variables were used for this analysis (Eq. (4)):

$$Y_t = \beta_0 + \beta_1 \cdot t + \beta_2 \cdot I(\text{River} - \text{Pre}) \cdot t + \beta_3 \cdot I(\text{River} - \text{Inhib}) \cdot t + \epsilon_t \quad (4)$$

Where Y_t is the quantitative variable that is considered (mean biofilm thickness or relative roughness coefficient), β_0 is the intercept, β_1 is the slope of the River-W case, β_2 is the difference in slope of the River-W and River-Pre and β_3 the difference in slope between River-W and River-Inhib. $I(\text{River-Pre})$ and $I(\text{River-Inhib})$ are the indicator variables (equal to 0 or 1 depending of the data set that is considered). T-test and

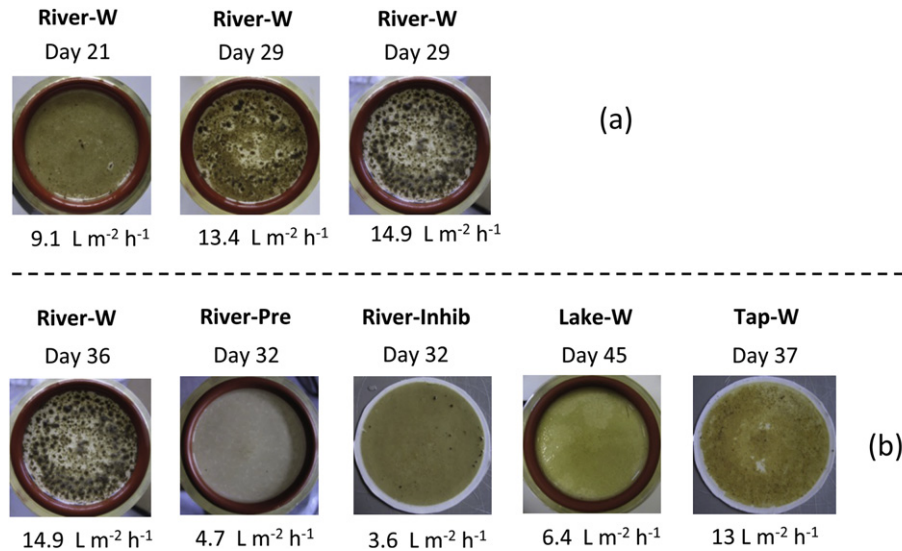


Fig. 3 – (a) Top view pictures of the biofilm developed on the same membrane in one River-W case at different stages of the experiment. (b) Top view pictures of the biofilm on the membrane for different feed water sources at a similar stage of the biofilm development. Flux data are normalized at 20 °C and expressed in $L m^{-2} h^{-1}$. The membrane diameter is 47 mm.

P-value calculations were then performed to statistically distinguish the different slopes that were calculated. A similar linear regression approach was also applied to statistically evaluate the effect of the water properties (in terms of presence/absence of metazoa and in terms of TOC content) on the predicted permeate flux.

2.4.3. Confocal laser scanning microscopy (CLSM)

The micro-scale structure of the biofilm was characterized using CLSM. First, membranes were sampled and fixed with formaldehyde solution (2.5%), washed twice with filtered Evian water and cut in sections of around $0.25 cm^2$. Then, biofilm samples were stained, incubated in the dark (4 h, 20 °C) and washed again. SYBR® Gold nucleic acid gel stain (1000 fold diluted stock solution, Invitrogen, Basel, Switzerland) was used to detect all microorganisms. Concanavalin A (50 fold diluted stock solution, Invitrogen, Basel, Switzerland) was used to stain the α -D-mannose and α -D-glucose groups of biopolymers. Alexa Fluor 514 was used as conjugate. Dehydration of the samples was then performed and consisted of six immersion steps of 20 min each in glycerol/water solutions with increasing glycerol/water content (40, 60, 80, 90, 95 and 100%). The fluorescence of SYBR® Gold was detected by excitation at 488 nm and emission at 495–540 nm. Concanavalin A was excited at 514 nm detected at an emission of 550–620 nm. The reflection from surfaces impermeable for light was detected at a wavelength of 633 nm using CLSM reflective mode. The Z-stacks were rebuilt in three dimensions with the software Imaris (Bitplane, Zürich, Switzerland). No quantification of microscale biofilm properties was performed based on CLSM images.

2.5. Permeate flux

The permeate flux was calculated by measuring the mass of water collected in each bottle and dividing the results by the filtration period and by the membrane area. The mass of

permeate was weighed daily using a scale (Ohaus Adventure Pro®, Pine Brook (NJ), USA). Flux measured in the Lake-W case was normalized to 20 °C using Eq. (5):

$$J_{20^\circ C} = \frac{J_T \cdot \mu_T}{\mu_{20^\circ C}} \quad (5)$$

where $J_{20^\circ C}$, J_T , $\mu_{20^\circ C}$ and μ_T indicate the corrected permeate flux at 20 °C ($L m^{-2} d^{-1}$), the measured permeate flux at room temperature ($L m^{-2} d^{-1}$), the water viscosity at 20 °C (Pa s) and the water viscosity at room temperature (Pa s), respectively. The kinematic viscosity depends on the temperature of the liquid and was computed with an empirical relationship (EPA, 2005):

$$\mu_T = 1.784 - (0.0575 \cdot T) + (0.011 \cdot T^2) - (10^{-5} \cdot T^3) \quad (6)$$

where T is the water temperature in °C and μ_T is the viscosity of water at temperature T in Pa s.

2.6. Characterization of protistan and metazoan diversity

The diversity of protistan and metazoan communities was characterized qualitatively by direct observations with a light microscope (Leica DMI 6000B fluorescence microscope or Zeiss Axio Imager equipped with 10×, 40× and 63× lenses). Multiple biofilm samples of about $0.6 cm^2$ were scratched from the membrane with the help of a scalpel and then re-suspended in $0.45 \mu m$ permeate water of the corresponding set-up (Whatmann, Maidstone, United Kingdom). Pictures of the detected organisms were recorded with cameras mounted on the microscopes (Leica DFC290 or Zeiss AxioCam). The observed organisms were allocated to different groups with the help of identification literature (e.g. Streble and Krauter, 1976). Protists were divided into “flagellates”, “ciliates”, “amoebae” and “heliozoans”, metazoa into “rotifers”, “nematodes” and “oligochaetes”.

2.7. Chemical analyses of carbon fractions

The TOC and Dissolved Organic Carbon (DOC) concentrations of the river and the tap water were measured by an automatic total organic carbon analyser (TOC-V, Shimadzu, Japan). The unfiltered samples were homogenized using a magnetic stirrer (Polytron PT 3100, 2 min with 15,000 rpm). Samples for DOC determination were filtered with a 0.45 µm membrane filter (Whatmann, Maidstone, United Kingdom). The analyser was calibrated with a stock solution composed of sodium nitrate (6.068 g L⁻¹), potassium hydrophthalate (2.126 g L⁻¹) and orthophosphoric acid (85%, 2 mL L⁻¹) dissolved in carbon-free water. To determine the TOC content of the biofilms, membranes were sampled and the entire biofilms detached by flushing 100 mL of nanopure water with the help of a sterile syringe. Since biofilms were flushed with significant amounts of nano-pure water, there were only insignificant quantities of DOC and thus TOC was equal to the particulate organic matter. Before determination, the unfiltered samples were homogenized with a mixer (Polytron PT 3100, Kinematica, Bohemia, NY, USA) (2 min with 15,000 rpm), a magnetic stirrer was added, and the sample was then closed using parafilm. Homogenization during injection ensured that the measurements were performed on a representative sample (avoiding sedimentation during injection into the TOC analyser).

Representative values for the AOC (Assimilable Organic Carbon) content of the feed water was taken from Hammes et al. (2010) and Lautenschlager et al. (2010) who evaluated the same water in an earlier study. In the Lake-W case the intake for the water samples was in 30 m depth (instead of 5 m depth for this study). Nevertheless these values give a good indication of the order of magnitude of AOC contents in the feed waters.

3. Results

3.1. Evaluation of the different bacterial growth capacities

Measurements of TOC, DOC and AOC are shown in Table 2. The lowest values were measured for tap water and the highest

values for river waters. Intermediate values were measured for lake water. Assuming a direct relation between TOC/DOC/AOC contents and bacterial growth, the bacterial growth capacity was the lowest for the tap water and the highest for the river water. A higher bacterial growth capacity induced a higher biofilm accumulation (Table 2). Biofilm concentrations of 0.2 g C m⁻² and of 0.6 g C m⁻² were measured for the Tap-W and Lake-W cases, respectively. Significantly higher biofilm concentrations were measured for systems operated with river water (values ranging from 1.8 to 8.7 g C m⁻²). The highest biofilm accumulation was found in the River-Inhib treatment (all predators inhibited) and the lowest for the River-Pre case (with pre-filtration of the river water). The influence of the pre-treatment of the water (anti-biotic or pre-filtration) on the biofilm accumulation will be discussed later.

3.2. Permeate flux

The change in the mean flux of each system was monitored for around 50 days of filtration (Fig. 2). For systems operated after 10 days at values ranging from 8 to 10 L m⁻² h⁻¹ and remained at this level until the end of the experiment. Mean fluxes measured in the Tap-W system continuously decreased for the first 25 days to stabilize at a level of 13–15 L m⁻² h⁻¹. In addition, we noted that the specific fluxes of the modules operated in the River-W system were scattered in a broad range after day 25 (from 4 up to 22 L m⁻² h⁻¹). Filtration performance was thus not correlated with substrate concentration in the feed water and amount of biofilm accumulated on the membrane.

3.3. Structure of the biofilms

The change in the biofilm physical structures was evaluated for each system at different spatial scales (i.e., macro-, meso- and micro-scale) using a conventional camera (top view images, Fig. 3a and b), OCT (Fig. 4) and CLSM (Fig. 5). These observations revealed that the biofilms developed in the River-W case were composed of the three main parts: (1) large and thick heterogeneities (in dark brown on the top view picture) (2) in the nearest neighbourhood of these heterogeneities, clean membrane surfaces with no biofilm are observed (in white on

Table 2 – Bacterial growth (expressed as TOC, DOC and AOC measurements) of the different feed water types from Chriesbach river, Lake Zurich and tap water. The number of analysed samples is shown in brackets next to the measurement value.

Water type	Feed water content			Biofilm concentration
	TOC ± std. error (# samples) (mg C L ⁻¹)	DOC ± std. error (# samples) (mg C L ⁻¹)	AOC ± std. error (# samples) (mg L ⁻¹)	TOC ± std. error (# samples) (g C m ⁻²)
River water (River-W)	3 ± 0.2 (19)	2.8 ± 0.2 (19)	0.3 ^a	6.0 ± 0.9 (3)
River water pre-filtered (River-Pre)	2.4 ± 0.1 (6)	2.3 ± 0.1 (5)	0.3 ^a	1.8 ± 0.7 (5)
River water with inhibition (River-Inhib)	2.8 ± 0.2 (14)	2.8 ± 0.2 (11)	0.3 ^a	8.7 ± 1.2 (3)
Lake water (Lake-W)	2 ± 0.1 (2)	1.5 ± 0.05 (2)	0.023 ± 0.02 ^a	0.6 (1)
Tap water (Tap-W)	0.9 ± 0.1 (4)	0.7 ± 0.03 (4)	0.002 ^b	0.2 ± 0.0 (2)

a (Hammes et al., 2010).

b From Lautenschlager et al. (2010).

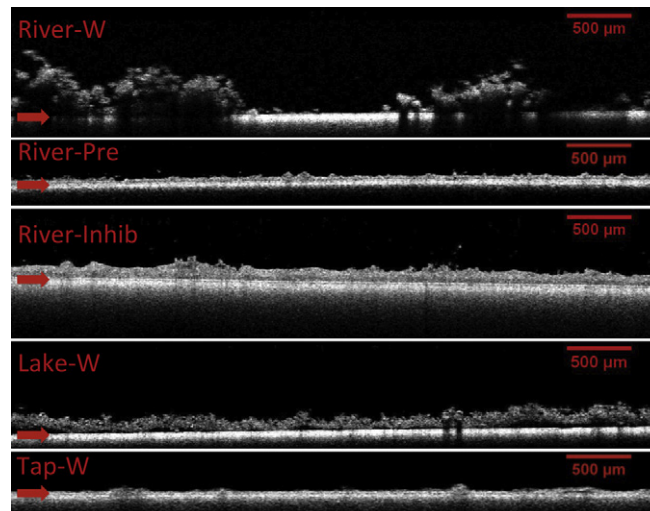


Fig. 4 – OCT pictures of the different types of biofilms. The scale bar is 500 μm . The images were taken after 51 days (River-W), 32 days (River-Pre), 43 days (River-Inhib), 64 days (Lake-W), or 37 days (Tap-W) of filtration. Arrows indicate the biofilm–membrane interface.

the top view pictures) and (3) a thin biofilm that developed far from the biofilm patches (in light brown on the top view picture). Biofilm structures observed in the other conditions (River-Pre, River-Inhib, Lake-W and Tap-W cases, i.e., in absence of metazoa) were smooth and homogeneous (Fig. 3b). No change in the biofilm structure was observed in these variants over time; full coverage of the membrane surface was noted from the beginning until the end of the experiments.

Quantifications of the membrane coverage (Fig. 6), of mean biofilm thickness (Fig. 7a) and of the relative roughness coefficient (Fig. 7b) were performed based on top view and OCT images using image analysis procedures as described in Section 2.4.2. Quantitative results confirmed the visual observation that the physical properties of River-W biofilms were significantly different from those of the other types of biofilms. Membrane coverage in the River-W case decreased from almost 100% to around 80% over 60 days of filtration reflecting a macro-scale change in the biofilm structure. Membrane coverage measured in the other variants remained high (close to 100% indicating full coverage of the membrane) during the entire period of experiment. In addition, River-W biofilms were thicker than other biofilms (Fig. 7a), which is likely due to their different morphology and higher biomass surface concentrations. The mean thickness of the River-W biofilms linearly increased to reach 200 μm after 60 days of filtration. Mean thicknesses of 100–150 μm were measured in the other variants at the end of the experiments. Relative roughness coefficients of 0.5–0.8 were calculated for the River-W biofilms whereas mean values of 0.25 were measured for all other types of biofilms. Statistical analysis was performed to evaluate the influence of the predation level on the change in the membrane coverage, mean biofilm thickness and in the relative roughness coefficient (Table 3). Slopes of the change in the different biofilm properties were different for the three cases (River-W, River-Pre, River-Inhib). The calculated *P*-values indicate that the slope for the River-Pre and River-Inhib treatments were statistically different from the slopes of

River-W treatment. This means that the physical properties of the biofilms developed with River-W were statistically different from those observed for the biofilms developed in the River-Pre and River-Inhib cases.

3.4. Predator diversity

Protistan and metazoan diversity in the different biofilms was characterized at different time between day 30 and day 60 except for the biofilms grown in the River-Inhib case (direct observations were done twice, at day 30 and 90) (Table 4). Based on these direct microscopic observations the River-W biofilms showed the highest organism diversity whereas the lowest diversity was observed for the Tap-W biofilms. In the River-W case flagellates were the dominant protists but some heliozoans, amoebae and ciliates were also observed. Metazoa were even more abundant than protists. Numerous rotifers, nematodes and oligochaetes were observed. Some larvae of Chironomidae were also observed. The community of the River-W biofilm was the only one that was characterized by the presence of metazoa. In the River-Pre Case, nematodes and oligochaetes were absent and very few rotifers were detected, which confirmed that pre-filtration was partly efficient to remove metazoa. Predominant protists were amoebae. Flagellates and heliozoans had also a rather high abundance in the biofilm. Inhibition of eukaryotes in the River-Inhib case was successful after 30 d of operation but partly successful after 60 d since a certain amount of living protists was observed. No metazoan organisms were however observed. Flagellates were the predominant organisms and some ciliates and amoebae were present. The predominant protists in the Lake-W biofilm community were amoebae. Ciliates and flagellates were present in small quantities. Metazoa were almost absent except for few rotifers but neither nematodes nor oligochaetes could be observed. Finally and as expected the abundance of protists and metazoa was

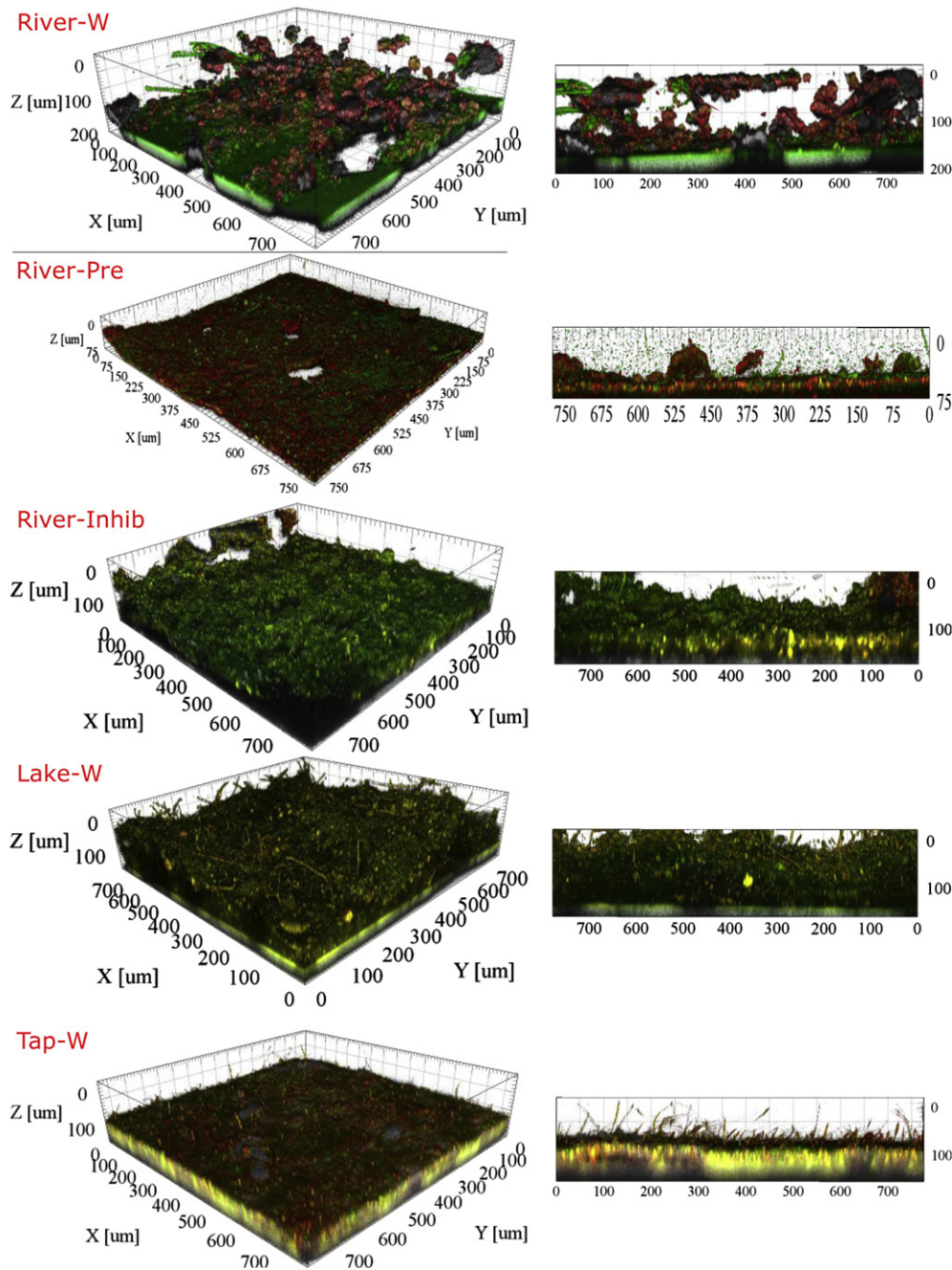


Fig. 5 – Three dimensional reconstructions of the Z-stacks acquired with the confocal microscope of the biofilm grown with the different feed waters after 42 days (River-W), 39 days (River-Pre), 30 days (River-Inhib), 45 days (Lake-W) and 37 days (Tap-W) of filtration, respectively. Green signal – SYBR® Gold stain, indicating presence of all biological cells; red signal – Concanavalin A stain, indicating presence of α -D-mannose and α -D-glucose groups in biopolymers (i.e., extracellular polymeric substance, EPS); grey signal – reflection of the solid surfaces. In the River-Pre case only the red and green signals are shown. The XY-dimension is 775 $\mu\text{m} \times 775 \mu\text{m}$. On the left side orthogonal views are illustrated. (For interpretation of the references to colour in this figure legend, the reader is referred to the web version of this article.)

very poor in the Tap-W biofilm. High abundance of Amoebae and flagellates were observed.

Statistical analysis was performed to test the hypothesis that the TOC and metazoan contents of the water govern the permeate flux (Table 5). Results of this statistical analysis (i.e., very small P-values) indicate that if the water source has

a significant TOC content or contains metazoa, the permeate flux will be statistically different from the one observed in absence of metazoa and for a low TOC content. Values of β_2 and β_3 indicate that an increasing TOC content decreases the permeate flux while the presence of metazoan tend to increase the permeate flux.

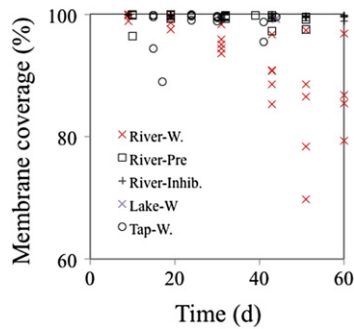


Fig. 6 – Change in the membrane coverage (%) measured for the different types of biofilm. Each data point corresponds to one biofilm.

4. Discussion

4.1. How do metazoa (nematodes and oligochaetes) engineer the biofilm structure?

In a previous study we demonstrated the significant influence of the presence/absence of predation during GDM filtration of creek river water (Derlon et al., 2012). However the eukaryotic populations that engineered the biofilm physical structure were not identified. In the current study we demonstrated that the eukaryotes that engineer the biofilm, physical structure are nematodes and oligochaetes. The main question is how nematodes and oligochaetes engineer the biofilm structure.

In the presence of nematodes and oligochaetes, biofilms were composed of thick and dense patches surrounded in their nearest neighbourhood by membrane surfaces free of biomass. Far from these biofilm patches, a thinner and ungrazed structure was observed (Figs. 3a and 4). Such biofilm patches are habitats built up by metazoa. A great number of nematodes indeed agglutinate detritus, thus forming lumps and burrows in the size range of few millimetres (Riemann and Helmke, 2002). The size of these habitats can range from several hundreds of microns to several millimetres as revealed by the observation of top view images in our study. At a higher trophic level, larvae of insects were also observed in some River-W biofilms. Larvae have the same capacity as nematodes to build specific habitats. In streams, larvae build oblong, tunnel-shaped retreats on stone surfaces (Stief and Becker, 2005). By forming these specific

Table 3 – Results of the statistical analysis of the influence of the predation level on the change in the membrane coverage, mean biofilm thickness and relative roughness coefficient. β_0 is the intercept, β_1 is the slope of the River-W case, β_2 is the difference in slope of the River-W and River-Pre and β_3 the difference in slope between River-W and River-Inhib.

	Estimate	Standard error	T-test	P-value
<i>Statistical analysis of the membrane coverage data</i>				
β_0	100.54	0.88	113.9	<2e-16
β_1 (River-W)	−0.28	0.02	−9.7	2.49e-15
β_2 (River-Pre)	0.18	0.03	6.2	1.82e-08
β_3 (River-Inhib)	0.19	0.02	8.4	9.52e-13
<i>Statistical analysis of the mean biofilm thickness data</i>				
β_0	−12.6	8.24	−1.5	0.13
β_1 (River-W)	3.3	0.21	15.5	<2e-16
β_2 (River-Pre)	−1.5	0.22	−6.7	2.92e-09
β_3 (River-Inhib)	−0.4	0.14	−2.8	0.00553
<i>Statistical analysis of the relative roughness coefficient</i>				
β_0	20.1	6.93	2.9	0.00543
β_1 (River-W)	0.76	0.18	4.3	7.02e-05
β_2 (River-Pre)	−0.72	0.16	−4.5	3.91e-05
β_3 (River-Inhib)	−0.55	0.16	−3.4	0.00146

structures, metazoa thus engineer the biofilm structure at the meso- and macro-scales and observations at the micro-scale using CLSM thus provide only limited information. The membrane surfaces free of biofilm that surrounded these retreats resulted from both the agglutination of detritus and from the overgrazing by metazoan organisms living in these protective habitats. Overgrazing and detritus agglutination by metazoa resulted in lower membrane coverage (due to the detection of “white” surface) and in higher mean thickness and relative roughness coefficient that can be quantified by image analysis. In our study the presence of metazoan activity increased by a factor of 2 the mean biofilm thickness and by a factor of 2–3 the relative roughness coefficient.

Biofilms do not only represent a habitat for nematodes but are also an important food resource (Majdi et al., 2011). In our study predation decreased the biofilm accumulation (reduction of 30% as compared to biofilm accumulation in the River-W and River-Inhib cases). Several studies reported that nematodes are opportunistic grazers. This implies that the diet of the nematodes is determined by the composition of the

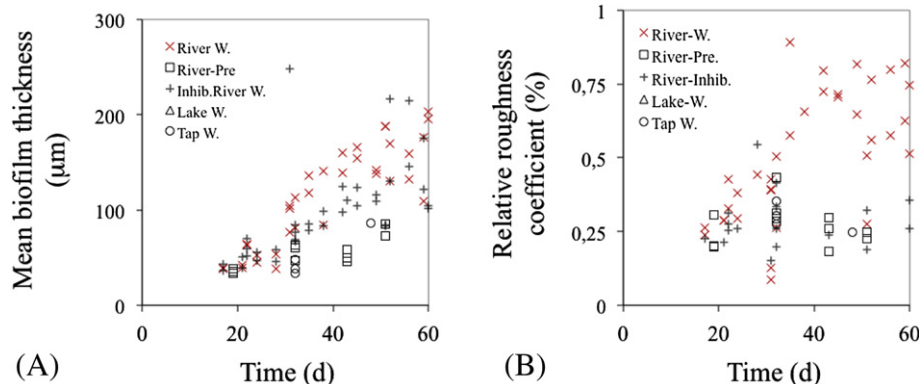


Fig. 7 – Change in the mean biofilm thickness (μm) and in the relative roughness coefficient (%) measured for the different types of biofilm based on OCT images. Each data point corresponds to one biofilm.

Table 4 – Presence and qualitative abundance of different protistan and metazoan groups in the biofilm grown with different water sources. +++ indicates predominant groups in a high abundance in the biofilm community, ++ an intermediate abundance and + the mere presence of the groups. – means that these organisms were not observed in the biofilm.

Water source	Protists				Metazoa		
	Flagellates	Ciliates	Amoebae	Heliozoans	Rotifers	Nematodes	Oligochaetes
River-W	+++	++	++	++	++	++	++
River-Pre	++	+	+++	++	+	–	–
River-Inhib	+++	++	++	–	–	–	–
Lake-W	+	+	+++	–	+	–	–
Tap-W	++	–	++	–	–	–	–

biofilms. Nematodes can graze on a wide range of food sources such as (i) green algae and cyanobacteria (Moens and Vincx, 1997), (ii) protozoans (Hamels et al., 2001), (iii) bacteria (Traunspurger, 1997) and (iv) EPS and organic detritus (Majdi et al., 2012). We can hypothesize that for biofilm developed during GDM filtration, the organic detritus that accumulate on the membrane surface represent the main food resource for the nematodes. The lower biofilm accumulation in the River-Pre case can be attributed to the removal of particulate matter by the pre-filtration and to the measurement that were performed at an earlier stage of biofilm growth.

Metazoan activity also influences the bacterial activity. Grazing by metazoa implies that the bacterial community is kept in an active growth phase, which induces a higher demand for nutrients. Higher demand for nutrients results in higher hydrolysis of particulate organic matter (De Mesel et al., 2003), which possibly enhances the biofilm permeability. Nematodes and oligochaetes secrete mucus (Riemann and Helmke, 2002). There is a relationship of commensalism between the mucus-secreting nematodes and the associated bacteria (Riemann and Helmke, 2002). Nematodes are believed to discharge hydrolytic enzymes into this mucus that hydrolyze, alone or together with the bacterial enzymes, organic particulate matter. The hydrolysed compounds, such as sugars, could then be directly consumed by bacteria, thus yielding extra nutrients directly from the detritus. The habitat of nematodes is conceived as an “enzymatic” reactor that is fuelled with detritus of the aggregate, but also suspended particulate matter and colloids it accretes (Riemann and Helmke, 2002).

All this different mechanisms associated to nematodes, oligochaetes and even insect larvae favour the development of highly heterogeneous biofilms that in turn enhances permeation. We could demonstrate that a modification of the predator community, e.g. removal of metazoa (River-Pre case), or a limited predator abundance (Tap-W case) is detrimental

to the process performance since it induced reduced filtration performances. By contrast, the presence of metazoa was beneficial to the system performances and operating conditions should aim at favouring this diversity. Overall our results demonstrate the importance of metazoa in terms of niche construction. Metazoa indeed engineered the environment in which they grew (i.e., the biofilm) into a more favourable habitat (i.e., patchy heterogeneous biofilm), which in turn resulted in a significant modification of the surrounding environment (i.e., the GDM system).

4.2. Combining GDM filtration with worms for the treatment of waters with high TOC content

In absence of predation, a higher TOC content of the feed water resulted in a lower permeate flux. The decrease of the permeate flux with an increasing TOC content is due to both a higher accumulation of particulate matter (originated from the influent) and a higher bacterial growth on soluble substrate. According to the equation of Carman-Kozeny the hydraulic resistance of a packed bed is a function of the porosity and thickness of the bed. Thus, the resistance of a biofilm is influenced by its structural parameters.

The filtration of water with high TOC content is not always associated with a low permeation flux and predation can help to develop a highly permeable biofilm that develops. From this observation, we can suggest that combining GDM filtration with removal of organic matter using worm-like organisms (e.g. oligochaetes or nematodes) is a suitable approach for the treatment of waters with high POC contents. Enhanced POC removal can be achieved by placing a worm reactor ahead of the filtration units or like in our case, by enhancing worm growth inside the filtration module itself. Worm reactors have also been investigated for the removal of excess sludge (Tamis et al., 2011). This technology consists in adding a worm reactor

Table 5 – Results of the statistical analysis of the influence of metazoa and TOC of the water source on the measured permeate flux. β_1 is the slope of the reference case (metazoa absent and low TOC content), β_2 is the difference in slope of the reference case and the case of high TOC content, and β_3 the difference in slope between the reference case and of the case of metazoa present.

	Estimate	Standard error	T-test	P-value
<i>Statistical analysis of the biofilm roughness data</i>				
β_1 (metazoa absent and low TOC content)	18.1	1	19.1	3.51e-15
β_2 (high TOC content)	–5.2	0.4	–11.9	4.84e-11
β_3 (metazoan present)	7.8	0.8	10.3	6.82e-10

on the recirculation loop and its application is often limited by the retention of the worms into the reactor. In GDM systems, worm retention would not be a problem due to the full retention by the membrane. Due to the absence of cross-flow conditions during GDM filtration, particle deposition is not size-dependant and all particles (and thus predators) entering the system then accumulate on the membrane surface.

Several types of worms are used to reduce excess sludge; free-swimming worms (e.g. *Aeolosoma* sp., *Nais* sp.) and crawling worms (e.g. *Tubificidae*, *Oligochaeta*), etc. *Lumbriculus variegatus* (*Oligochaeta*, *Lumbriculidae*) has been extensively used since this species has the higher potential to reduce sludge (Buys, 2005) but is rarely present in wastewater, and widely found in natural water bodies in Europe and North-America (Elissen et al., 2006). *Lumbriculus variegatus* would thus be a perfect candidate to reduce organic matter during GDM filtration of surface waters. Some other species like *Aulophorus furcatus* are naturally present in activated sludge (Tamis et al., 2011) and would thus be more adapted to treatment of surface water with high TOC content. In our study, worms were naturally present in the river water and no specific inoculation was required. In the lake water variant, worms were absent but this is likely due to the sampling point (5 m deep but 1 m above the sediments).

GDM filtration of water with high TOC and combined with removal of organic matter using worms appear thus feasible due to: (1) the full retention of worms, (2) the horizontal immobilization of the worms, (3) the existence of worm species adapted to high organic pollutant concentration like in activated sludge, and (4) the absence of inhibition by ammonium concentration.

5. Conclusions

- i. Biofilm formation on membranes can be a major cause of flux decline. We were able to demonstrate that, at low transmembrane pressure and in absence of control of the biofilm formation, the composition of the microbial community (bacteria and predators) is as important as the amount of organic substrate in the feed water.
- ii. High permeate flux was maintained during GDM filtration of waters with high TOC content due to the presence of predation by metazoa that increased the hydraulic permeability of the biofilm. Thick but open and heterogeneous biofilm structures developed in presence of metazoa.
- iii. In the absence of predation by metazoan organisms, the hydraulic permeability of the biofilm is governed by the TOC content only. Under these conditions, the permeate flux is inversely related to TOC content due to higher accumulation of biofilm.
- iv. Enhancing POC removal with worms before ultrafiltration units appears suitable for the treatment of surface water with high POC content.

REFERENCES

- Arnal, J.M., Garcia-Payos, B., Verdu, G., Lora, J., Sancho, M., 2008. AQUAPOT: study of the causes in reduction of permeate flow in spiral wound UF membrane. Simulation of a non-rigorous cleaning protocol in a drinkable water treatment facility. *Desalination* 222 (1–3), 513–518.
- Butler, R., 2009. Skyjuice technology impact on the UN MDG outcomes for safe affordable potable water. *Desalination* 248 (1–3), 622–628.
- Buys, B.R., 2005. Personal Communication. Wageningen University and Research Centre, The Netherlands.
- De Mesel, I., Derycke, S., Swings, J., Vincx, M., Moens, T., 2003. Influence of bacterivorous nematodes on the decomposition of cordgrass. *Journal of Experimental Marine Biology and Ecology* 296 (2), 227–242.
- Derlon, N., Peter-Varbanets, M., Scheidegger, A., Pronk, W., Morgenroth, E., 2012. Predation influences the structure of biofilm developed on ultrafiltration membranes. *Water Research* 46 (10), 3323–3333.
- Elissen, H.J.H., Hendrickx, T.L.G., Temmink, H., Buisman, C.J.N., 2006. A new reactor concept for sludge reduction using aquatic worms. *Water Research* 40 (20), 3713–3718.
- EPA, 2005. Membrane Filtration Guidance Manual. United States Environmental Protection Agency. Office of Water 4601(332).
- Hamels, I., Moens, T., Mutylaert, K., Vyverman, W., 2001. Trophic interactions between ciliates and nematodes from an intertidal flat. *Aquatic Microbial Ecology* 26 (1), 61–72.
- Hammes, F., Goldschmidt, F., Vital, M., Wang, Y., Egli, T., 2010. Measurement and interpretation of microbial adenosine triphosphate (ATP) in aquatic environments. *Water Research* 44 (13), 3915–3923.
- Lautenschlager, K., Boon, N., Wang, Y., Egli, T., Hammes, F., 2010. Overnight stagnation of drinking water in household taps induces microbial growth and changes in community composition. *Water Research* 44 (17), 4868–4877.
- Majdi, N., Traunspurger, W., Boyer, S., Mialet, B., Tackx, M., Fernandez, R., Gehner, S., Ten-Hage, L., Buffan-Dubau, E., 2011. Response of biofilm-dwelling nematodes to habitat changes in the Garonne River, France: influence of hydrodynamics and microalgal availability. *Hydrobiologia* 673 (1), 229–244.
- Majdi, N., Tackx, M., Traunspurger, W., Buffan-Dubau, E., 2012. Feeding of biofilm-dwelling nematodes examined using HPLC-analysis of gut pigment contents. *Hydrobiologia* 680 (1), 219–232.
- Moens, T., Vincx, M., 1997. Observations on the feeding ecology of estuarine nematodes. *Journal of the Marine Biological Association of the United Kingdom* 77 (1), 211–227.
- Peter-Varbanets, M., Hammes, F., Vital, M., Pronk, W., 2010. Stabilization of flux during dead-end ultra-low pressure ultrafiltration. *Water Research* 44 (12), 3607–3616.
- R Development Core Team, 2011. R: A Language and Environment for Statistical Computing, Vienna, Austria [online]. <http://www.R-project.org/>.
- Riemann, F., Helmke, E., 2002. Symbiotic relations of sediment-agglutinating nematodes and bacteria in detrital habitats: the enzyme-sharing concept. *Marine Ecology-Pubblicazioni Della Stazione Zoologica Di Napoli I* 23 (2), 93–113.
- Stief, P., Becker, G., 2005. Structuring of epilithic biofilms by the caddisfly *Tinodes rostocki*: photosynthetic activity and photopigment distribution in and beside larval retreats. *Aquatic Microbial Ecology* 38 (1), 71–79.
- Streble, H., Krauter, D., 1976. *Das Leben im Wassertropfen*. Frankh'sche Verlagshandlung, W. Keller & Co, Stuttgart.
- Tamis, J., van Schouwenburg, G., Kleerebezem, R., van Loosdrecht, M.C.M., 2011. A full scale worm reactor for efficient sludge reduction by predation in a wastewater treatment plant. *Water Research* 45 (18), 5916–5924.
- Traunspurger, W., 1997. Bathymetric, seasonal and vertical distribution of feeding-types of nematodes in an oligotrophic lake. *Vie Et Milieu-life and Environment* 47 (1), 1–7.